



NATIONAL TRANSPORTATION SAFETY BOARD
Investigative Hearing

Norfolk Southern Railway general merchandise freight train 32N
derailment with subsequent hazardous material release and fires,
in East Palestine, Ohio, on February 3, 2023

GROUP	E
EXHIBIT	
7	

Agency / Organization

Rail. Eng. Science

Title

**Exhibit 7- Tarawneh, RES,
March 20212012**



Defect detection in freight railcar tapered-roller bearings using vibration techniques

Constantine Tarawneh¹ · Joseph Montalvo¹ · Brent Wilson²

Received: 31 August 2020/Revised: 13 December 2020/Accepted: 22 December 2020/Published online: 3 February 2021
© The Author(s) 2021

Abstract Currently, there are two types of defect detection systems used to monitor the health of freight railcar bearings in service: wayside hot-box detection systems and trackside acoustic detection systems. These systems have proven to be inefficient in accurately determining bearing health, especially in the early stages of defect development. To that end, a prototype onboard bearing condition monitoring system has been developed and validated through extensive laboratory testing and a designated field test in 2015 at the Transportation Technology Center, Inc. in Pueblo, CO. The devised system can accurately and reliably characterize the health of bearings based on developed vibration thresholds and can identify defective tapered-roller bearing components with defect areas smaller than 12.9 cm² while in service.

Keywords Railcar health monitoring · Onboard condition monitoring systems · Bearing defect detection · Bearing vibration signatures · Bearing spectral analysis

1 Introduction

The cargo load of each freight railcar is supported by the railcar's suspension components: springs, dampers, axles, wheels, tapered-roller bearings, and side frames. Of these components, the bearings are the most susceptible to failure due to the heavy cargo loads they support at high speeds.

The tapered-roller bearing typically used in freight railcar service has three distinct fundamental components: rollers, inner rings (cones), and outer ring (cup). These components, shown in Fig. 1, allow for near-frictionless operation under heavy loads and high speeds. However, when one of these components develops a defect, the operational effectiveness is compromised, which may lead to increased frictional heating depending on the size and location of the initiated defect.

The defects can be categorized into one of three general categories: a geometric defect, a localized defect, or a distributed defect. A geometric defect is when one or more of the fundamental components of the bearing are out of tolerance because of inconsistencies in the manufacturing processes. A bearing can also develop a geometric defect through improper reconditioning or prolonged usage. Two examples of localized defects that include pits, cracks, or spalls on a single component of the bearing are illustrated in Fig. 2 (left). A distributed defect is when multiple bearing components have localized defects or a single component with multiple defects that are distributed throughout its surface such as a water-etch defect, pictured in Fig. 2 (right). Water-etch is the consequence of water entering the bearing through an orifice or broken seal and degrading the grease. This grease degradation leads to increased metal-to-metal friction, which in turn causes the rolling surfaces of the bearing components to wear away at

✉ Constantine Tarawneh
constantine.tarawneh@utrgv.edu

¹ University Transportation Center for Railway Safety (UTCRS), University of Texas Rio Grande Valley (UTRGV), Edinburg, TX, USA

² Hum Industrial Technology, Inc, St. Louis, MO, USA

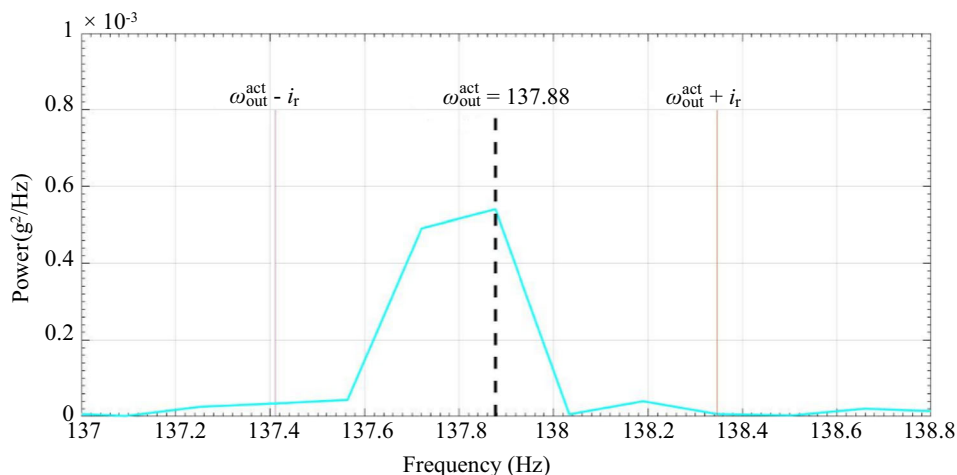


Fig. 16 Example of using the integration ranges to calculate the normalized defect energy for each fundamental defect frequency

5 Results and discussion

To demonstrate the efficacy of the proposed onboard condition monitoring system, validation testing examples that were obtained from both laboratory and field testing at TTCI are given hereafter. In the first example, a bearing with a defective outer ring (cup) that was tested in the laboratory is presented, whereas, in the second example, a bearing with a defective inner ring (cone) that was field tested at the TTCI rail tracks is examined. These examples were carefully chosen to showcase the effectiveness and accuracy of the proposed system in identifying relatively small defects that are in their early stages of development both in a laboratory setting and in field service.

To obtain one representative value for each speed and load combination during laboratory testing, the mean of the RMS and NDE values for the final 2 h of data acquired (i.e., twelve data points) were calculated for Level 1 and Level 2 analyses, respectively. In field testing, the latter was accomplished by obtaining the mean of all the RMS and NDE values after speed reached steady state. All Level 1, Level 2, and temperature results will be summarized in tables. RMS values above the T_p in the Level 1 tables will be italicized, whereas the RMS values above the T_{max} in Level 1 tables and percentages of the NDE values above 50% in Level 2 tables will be bolded.

5.1 Laboratory experiment 200: cup defect

In laboratory Experiment 200, a class K bearing with a pitted inboard cup (outer ring) raceway was run in the B2 position on the 4BT (refer to Fig. 5). The initial defect, pictured in Fig. 17 (left), propagated throughout the experiment to a final size of 8.98 cm² (1.39 in²), as shown in Fig. 17 (right).

The final defect size of 8.98 cm² corresponds to approximately 2.4% of the 367.28 cm² (56.93 in²) total area of one cup raceway in a class K bearing. To accelerate the testing and simulate a worst-case scenario, the region of the pit on the cup was placed directly under the full load path and the bearing was run at 137 km/h (85 mph) and 110% of full load representing an overloaded railcar.

5.1.1 Level 1 analysis: Is the bearing defective?

Figure 18 depicts the vibration and temperature profiles for bearing 2 (B2) and bearing 3 (B3) throughout Experiment 200. The control bearing correlation in Fig. 18 refers to a previous study for which the average operating temperatures above ambient (ΔT) for healthy (defect-free) bearings at several speeds for empty and fully loaded railcars were acquired [7]. Note that bearings tend to operate at temperatures above the control bearing threshold regardless of bearing health at the beginning of experiments as the freshly packed grease breaks in. The ambient temperature was held at 20 °C (68 °F). Tables 5 and 6 provide the average values of the final 2 h of each loading condition during the experiment.

Initially, the vibration levels within B2 were slightly below the T_{max} . After the 150-h mark, B2 vibration levels started to increase reaching levels that are noticeably above the T_{max} , signifying a defective bearing. This fluctuation in vibration levels is indicative of defect growth. As the defect grows, metal debris from the cup raceway is circulated throughout the bearing during operation. This causes an increase in roller misalignment and is represented by an increase in vibration. However, as the debris gets crushed by the rotating rollers, the vibration levels start to decline. This cycle repeats itself every time the defect deteriorates. Since the vibration levels within B2 exceeded the T_{max} at

137 km/h (85 mph), B2 proceeds to Level 2 analysis. The vibration levels within B3 remained above the T_p but below the T_{max} . Upon teardown and visual inspection, B3 did not have any visible defects and was determined to be healthy.

5.1.2 Level 2 analysis: What is the defect type?

Since B2 was classified as defective in Level 1 analysis, the NDE (“max/sum”) value is calculated. The results in Table 7 show the Level 2 analysis for B2 using the proposed method in Eq. (13). The analysis performed at a simulated train speed of 137 km/h (85 mph) and 110% of full load resulted in a NDE_{cup} of 99.6%, which confirms that the bearing has a defect on its cup (outer ring) raceways. Consequently, the analysis proceeds to Level 3 in which the defect size is estimated using the developed defect size correlations [18].

5.2 Field test validation

To demonstrate the efficacy of the proposed onboard condition monitoring system in rail service, it was implemented in a field test performed at the TTCI rail tracks as described in Sect. 3.4 of this paper. This field test was successful, and the individuals performing the analysis of the acquired data were able to accurately identify all four defective bearings as well as the location of the defect (i.e., whether it is on the cone or cup of the bearing). The analysis performed on the bearing located in the L1 position (refer to Fig. 11 and Table 3) is presented here. This bearing had a defective cone (inner ring) with a total spalled area of 14.2 cm² (2.2 in²), as pictured in Fig. 19. This bearing was chosen because current wayside detection systems are not proficient in identifying cone defects. Hence, being able to reliably detect cone spalls in rail service is advantageous. Photographs of the defective cone in the L1 Bearing are shown in Fig. 19. Test speeds varied between 64 km/h (40 mph) and 105 km/h (65 mph), and test loads alternated between 17% (empty railcar) and 100% (fully loaded freight railcar).

5.2.1 Level 1 analysis: Is the bearing defective?

Table 8 provides a summary of the percentages of steady-state data that were found to have RMS values above the T_{max} for each speed and load iteration. The results show that the L1 Bearing was accurately classified as defective in

almost all the steady-state data acquired during the TTCI field test for every load and speed combination. The lack of data acquired at full load and speeds above 89 km/h (55 mph) is because the testing facility at TTCI limited the speed of fully loaded railcars to no more than 89 km/h (55 mph). Since the bearing was correctly identified as defective, the analysis proceeds to Level 2 to identify the defective component within the bearing assembly.

5.2.2 Level 2 analysis: What is the defect type?

Level 2 analysis was performed on the defective L1 Bearing. A summary of the results under unloaded and fully loaded conditions are provided in Table 9. From the results, it is evident that the algorithm has correctly identified the defective component within the bearing for all speed and load iterations. The data also suggest that the normalized defect energy (NDE) for the defective component increases with load and speed. This means that the algorithm is proficient in identifying defective bearings and the type of defect within the bearing at higher speeds and full load.

6 Conclusions and future work

Wayside condition monitoring systems currently in use in North America are reactive in nature, and numerous derailments have resulted from overheated bearings that went undetected. To combat this, an onboard bearing condition monitoring system was developed that can accurately and reliably detect bearings with surface defects smaller than 4% of the total raceway surface area by analyzing the vibration signatures emitted by the bearings.

The devised onboard condition monitoring system has undergone rigorous laboratory testing and targeted field testing at the Transportation Technology Center, Inc. (TTCI) at Pueblo, Co. A wireless version of the system has also been developed and tested extensively yielding results identical to those of the wired version. The authors are working with a private rail industry partner to deploy this wireless system in a couple of Class I and II railroads and gather data to further validate the efficacy and accuracy of the system in detecting defective bearings in regular rail service. Moreover, the acquired vibration data from these planned field tests will be correlated to wheel impact load detector (WILD) data to determine whether the onboard

Table 7 Level 2 analysis of Bearing 2 for Experiment 200 using NDE

Track speed (km/h)/(mph)	Load (%)	NDE $\frac{\max}{\text{sum}} \times 100\%$	Defective component
137/85	110	99.6	Cup